13

Ni-based multilayer structures for Goebel-type mirrors

© K.V. Durov, V.N. Polkovnikov, N.I. Chkhalo, A.A. Akhsakhalyan, I.V. Malyshev

Institute of Physics of Microstructures, Russian Academy of Sciences,
603950 Nizhny Novgorod, Russia
e-mail: zevs2801@mail.ru

Received May 7, 2024
Revised May 7, 2024
Accepted May 7, 2024

In this work, the characteristics of the $Ni_{80}Mo_{20}$/Si multilayer structure, which is promising for the manufacture of Goebel mirrors, were studied for the first time. The structural parameters of the multilayer structure were determined. It is shown that the values of the transition regions for $\sigma(Ni_{80}Mo_{20})$ and $\sigma(Si)$ are 5 and 8.5 Å angstroms, respectively. The composition of the structures was found at which the best reflectivity $R = 69.5-56.1\%$ was achieved for periods of $41.5-32$ Å angstroms.

Keywords: multilayer X-ray mirrors, magnetron sputtering, Goebel mirrors.

DOI: 10.61011/TP.2024.08.59005.149-24

Introduction

An important step in the field of creation of elements for focusing or collimating X-ray beams for linear sources was made when Göbel [1] proposed and experimentally implemented systems for forming gradient multilayer structures deposited on the surfaces of elliptical and parabolic cylinders. The period of such a structure varies along the cylinder guide so that the Wolf-Bragg condition $2d \sin\theta = \lambda$ is satisfied at each point of the surface, where d is the period of the multilayer structure, θ is the radiation slip angle, and λ is the radiation wavelength. Such mirrors are most broadly used for collimating and focusing hard X-ray radiation at $\lambda \approx (0.05-0.25\,\text{nm})$ from linear anodes of X-ray tubes. The use of such mirrors made it possible to increase the efficiency of X-ray tube radiation selection by more than an order of magnitude. Currently, almost all modern diffractometers, X-ray fluorescence analysis devices and other X-ray equipment of technical and scientific applications are provided with such mirrors.

W/Si is a widely used pair of materials for Goebel mirrors [2,3]. These mirrors have relatively high (above 70%) reflection coefficients at a wavelength of 0.154 nm (CuK_α radiation). However,when such structures are used, the quasi-Bragg scattering of the CuK_β line with $\lambda = 0.139$ nm appears, which was predicted theoretically in Ref. [4] and it was earlier experimentally observed in Ref. [5]. This effect is related to interference amplification of the intensity of scattered waves from correlated interfaces. Coherent repetition of rough interfaces from layer to layer results in the resonant amplification of diffuse X-ray scattering, generating the so-called quasi-Bragg band under the modified Wolf-Bragg condition

$$\lambda = d(\sin\theta_{\text{in}} + \sin\theta_{\text{sc}}) = 2d\sin\theta_{\text{Br}}, \qquad (1)$$

where λ — the wavelength of the X-ray photon, d — the period of the multilayer X-ray mirror, θ_{in} and θ_{sc} — the grazing and scattering angles, respectively, θ_{Br} — the Bragg angle. The expression (1) is a condition for the occurrence of a diffraction maximum in case of scattering on a lattice whose inverse vector coincides with the inverse vector of a multilayer X-ray mirror. In other words, the occurrence of quasi-Bragg scattering is attributable to the fact that the roughness being reproduced from layer to layer forms a „lattice".

This phenomenon can result in incorrect identification of additional peaks that will appear during diffractometric measurements. Therefore, there is a natural question about the suppression of the radiation line CuK_β.

In most cases, when using X-ray tubes as sources of X-ray radiation, this problem is easily solved by using a filter that is made of a lighter anode material that is closest to the one used in the X-ray tube. For example, this is Ni for Cu. Ni absorption line — $\lambda = 0.149$ nm. Thus, this material has high transmittance at $\lambda > 0.149$ nm and low transmittance at $\lambda < 0.149$ nm. That is, this step can ensure the suppression of the intensity of CuK_β-lines in case of usage of Cu-based anode. Calculations show that the degree of suppression can reach two orders of magnitude. However, together with the suppression of spurious radiation, the filter will result in a drop of the intensity of the useful signal. In addition, the use of a free-hanging filter results in a complication of the device circuit and to some difficulties in operation: filters are quite fragile, since they comprise films with a thickness of about 100 nm. Therefore, instead of introducing filters, it is worth considering the option of replacing the reflective coating based on a pair of W/Si materials.

Since nickel has characteristics that make it possible to suppress the CuK_β radiation line, multilayer X-ray mirrors based on this material look promising for the problems under consideration. For example, Ni/Si, Ni/C, $Ni_{80}Mo_{20}$/Si, and $Ni_{80}Mo_{20}$/C. Here, „light" materials such as silicon Si and carbon C, which are sufficiently transparent in

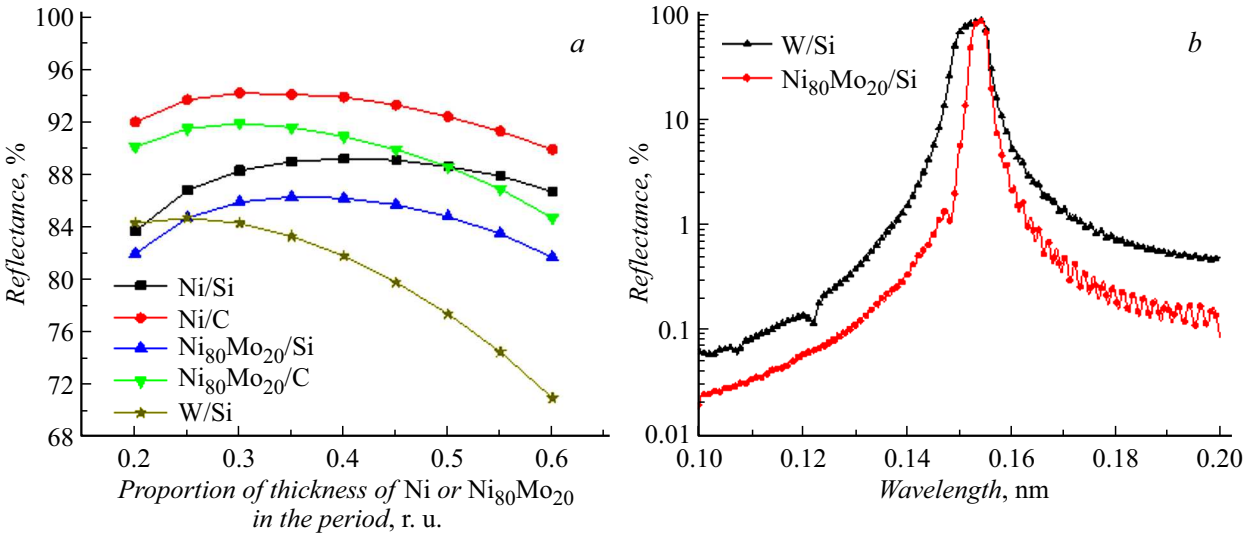

Figure 1. Calculated reflection coefficients in the first order of diffraction on $\lambda = 0.154$ nm of Ni-containing mirrors depending on the thickness Ni (a) and spectral dependences for W/Si and $Ni_{80}Mo_{20}$/Si with the share of W and $Ni_{80}Mo_{20}$ in the period of $\beta = 0.25$ (b).

the wavelength range under consideration, are chosen as optically contrasting materials with respect to nickel. The notation of $Ni_{80}Mo_{20}$ corresponds to an alloy of nickel and molybdenum (80% nickel to 20% molybdenum).

Fig. 1, *a* show the results of calculations of reflection coefficients in the first order of diffraction from the corresponding structures with perfectly smooth and sharp material interfaces. Mirror periods in calculations $d = 4$ nm, the number of periods in structures is $N = 100$. Calculations were performed in „Multifitting“ [6] program using optical constants from the CXRO database [7].

Existing methods for the synthesis of multilayer structures, in particular magnetron sputtering, do not allow achieving ideal interfaces. In practice, chemical interaction and diffusion of material atoms reduce the optical contrast in a multilayer structure, and significant interlayer roughness leads to diffuse scattering of radiation. Both of these effects negatively affect the reflectivity of the multilayer X-ray mirror. Therefore, there is an interest in studying the real boundaries of the claimed structures.

Multilayer mirrors based on Ni/C and Ni/Si were studied, for example, in Ref. [8–10]. However, here the main attention was drawn to the reflective and other properties of these mirrors in the soft X-ray range. Nevertheless, the authors were able to determine the values of interlayer roughness (about 0.25–0.30 nm), on the basis of which it is possible to perform a theoretical prediction of the reflective properties of these mirrors in the hard X-ray range.

We study the reflective properties and structural characteristics of the $Ni_{80}Mo_{20}$/Si multilayer structure in this paper. The choice is determined by the properties of the $Ni_{80}Mo_{20}$ alloy. Unlike pure Ni, its alloy with Mo (at 20% molybdenum) is not magnetic. This is important for the case of magnetron sputtering of structures, since a non-magnetic target does not distort the magnetic field of magnetrons and, accordingly, the typical distribution of the flow of matter over the target. Such structures have not been studied before.

Regarding the suppression of the CuK_β line, theoretical spectral reflectivity dependences for W/Si and Ni_{80}MoIFx1x1xE/Si mirrors (Fig. 1, *b*) were plotted in „Multifitting“ program. Despite the comparable reflection on the CuK_α line (84.6%), in the case of W/Si, the reflection of the CuK_β line is 4.5 times higher than that of $Ni_{80}Mo_{20}$/Si.

1. Experimental method

Multilayer $Ni_{80}Mo_{20}$/Si structures were synthesized by direct current magnetron sputtering on a setup provided with two magnetrons in the course of experiments. Round planar magnetrons have an erosion zone with a diameter of 110 mm. The residual gas pressure in the chamber was 10^{-6} mbar before the process. High-purity (99.998%) argon was used as the working gas, the pressure of which during the sputtering process was $(1.0–1.3) \cdot 10^{-3}$ mbar. The magnetrons were powered by stabilized current sources developed in IPM RAS. The current values were 300 mA for $Ni_{80}Mo_{20}$ and 400 mA for Si during the entire process. The film growth rates were maintained at 0.12 nm/s for $Ni_{80}Mo_{20}$ and 0.07 nm/s for Si.

The root-mean-square interlayer roughness of the initial surfaces should be at the level of $\sigma \approx (0.1–0.3)$ nm and below for obtaining relatively high reflection coefficients from a multilayer structure in the X-ray range. In our study, flat silicon substrates ($\sigma \approx 0.2$ nm) with a size of 25×25 mm, pre-cut from a single round plate with a diameter of 100 mm and a thickness of 0.46 mm, were used as substrates for the microelectronic industry. The substrates were mounted vertically on a holder that performed a reciprocating motion over the magnetrons during sputtering.

Changing of the speed of the holder passing over the magnetrons allowed adjusting the thickness of the layer applied to the substrate in one pass. Thus, layer-by-layer application of materials was carried out.

As a rule, the flow of the sputtered substance from the target surface is uneven. The maximum flow density is located above the center of the circular target. Therefore, precision shaped diaphragms were installed between the magnetrons and the substrate for creating the uniform coatings, the slits of these diaphragms allow controlling the distribution of the flow of matter onto the substrate. The specific type of precision diaphragms for each target was determined experimentally. The uniformity of films on the substrate surface was 0.4% in our experiments.

The reflectance characteristics of the multilayer structures were measured using a four-crystal laboratory diffractometer PANalitycal X'Pert PRO MRD, which makes it possible to apply the method of small-angle X-ray reflectometry. The sample was placed on a table with six degrees of freedom. An X-ray tube was a source of X-ray radiation with a wavelength of $\lambda = 0.154\,\text{nm}$ (Cu lineK_α). The operating parameters of the X-ray tube were as follows: voltage $U = 30\,\text{kV}$, electron beam current $I = 20\,\text{mA}$. Spectral and angular monochromatization of the probe beam was performed using a four-crystal asymmetric monochromator Ge (220). Exit slits further behind the monochromator limited the beam in the horizontal and vertical planes. A holder with a Soller collimator and an inlet slit are installed in front of the gas proportional detector.

The values of the reflection coefficients given in this paper were determined as the ratio of the radiation intensity (number of photons per second) reflected from the mirror to the intensity of the reference signal. We can talk about the error of the determined values of the reflection coefficients in $\pm 1\%$ due to the sufficient exposure time and small statistical fluctuations of photons from the source and electrons in the detector.

The interfaces of this multilayer structure cannot be perfect due to various physical processes that occur during the sputtering of X-ray mirrors. The effect of interlayer roughness and mixing (diffusion and chemical interaction of materials) leads, respectively, to radiation scattering and a decrease of the sharpness of the permittivity profile, and, as a consequence, to a decrease of the reflectivity of the mirror. At the same time, it is important to understand exactly what parameter caused this decrease, since this further determines the choice of a method for improving interfaces that suppresses the development of either roughness or mixing. Therefore, angular dependences of mirror reflection and diffuse scattering coefficients were measured to discriminate the contributions of interlayer roughness and mixing of materials.

The sample was adjusted so that the X-ray beam was divided in half for obtaining the mirror reflection curve. This angular position was taken as zero. The radiation source remained stationary, and the detector, turning at an angular velocity twice as fast as the sample, recorded the intensity of the radiation reflected by the sample.

Diffuse scattering curves were obtained as follows: the sample and detector were positioned relative to a stationary radiation source at an angle corresponding to the first Bragg peak, after which the intensity of scattered radiation was measured at different angles of rotation of the sample. The position of the detector remained fixed in this case.

The parameters of X-ray mirrors (periods, thicknesses of material layers and mixed regions, as well as interlayer roughnesses) were determined by fitting mirror reflection and diffuse scattering curves using program „Multifitting“ for reflectometric reconstruction of multilayer structures developed in IPM RAS. It makes it possible to calculate the spectral and angular dependences of the reflection coefficient on the simulated structure by solving a system of recurrent relations, as well as to simultaneously fit several experimental curves taken in different spectral ranges.

A linear growth model [11] was used to calculate the roughness of the boundaries. The power spectral density function (PSD function) of interfaces is partially inherited in this model from the previous models and is partially replaced by the growth model:

$$\text{PSD}_{2D}(\nu) = \text{PSD}_{\text{sub}}(\nu)\exp\big(-b(\nu)h\big) + \Omega\big[(1-\exp\big(-b(\nu)h\big))/\exp\big(-b(\nu)h\big)\big], \qquad (2)$$

where ν is the spatial frequency, $\text{PSD}_{\text{sub}}(\nu)$ corresponds to the substrate, $\exp(-b(\nu)h)$ is the inheritance factor, $b(\nu)$ is the surface relaxation function, which is represented as a polynomial in degrees of spatial frequency, h is the layer thickness, Ω is the volume of particles (atoms, molecules, or clusters) falling during growth. The ABC model [12] was chosen as the model describing the PSD function of the substrate in the formula (2). In this case, it is described by the following expression:

$$\text{PSD}_{\text{sub}}(\nu) = 4\pi\sigma^2\alpha/(1+\xi^2(2\pi\nu)^2)^{\alpha+1}, \qquad (3)$$

where σ is the total root-mean-square roughness height of the substrate, for frequencies from 0 to $+\infty$, α is the fractal dimension that determines the rate of spectrum decay to the high-frequency region, ξ is transverse (along the layer) correlation length. The value of the interlayer roughness of layers was obtained after substituting (3) into the PSD function of interfaces and integrating it in a given range of spatial frequencies, which was determined from the condition $2\pi\nu = k(\cos\theta_0 - \cos\theta)$, where ν is the value of the spatial frequency, θ_0 is the angle corresponding to the mirror reflection is θ is the scattering angle, and k is the wavenumber. The value of the scattering angle close to the position of the Bragg peak was chosen to obtain the lower bound of integration, and the value corresponding to the maximum scattering angle was chosen to obtain the upper bound.

Parameters of synthesized multilayer structures $PNi_{80}Mo_{20}/Si$

Sample	KD-121	KD-122	KD-123	KD-124	KD-125	KD-126	KD-127	KD-128
N	60	60	60	60	60	60	60	60
d, Å	41.24	42.20	43.60	41.28	43.33	40.93	42.86	42.68
β, a.u.	0.580	0.480	0.432	0.418	0.368	0.363	0.326	0.265
$\sigma(Ni_{80}Mo_{20})$, Å	4.8	4.7	5.6	5.0	5.8	4.6	5.0	4.5
σ(Si), Å	11.2	9.7	8.1	8.7	8.4	8.8	8.8	9.9
R, %	32	58	62	62	65	62	64	62

2. Results and discussion

At the first stage of the study, the optimal structure parameters were searched for, at which their best reflectivity was achieved. A number of $Ni_{80}Mo_{20}/Si$ structures with different ratios of material layer thicknesses were synthesized for this purpose. We tried to keep the number of periods and the period value itself unchanged at the same time. The values of periods at the extreme points typical for Goebel mirrors were taken as a basis: $d \approx 41.5$ and 33.5 Å. They correspond to the grazing angles $\theta \approx 1.106$ and 1.355° for a mirror length of 40 mm, the distance from the mirror center to the linear focus of the X-ray tube of 100 mm, and the cylinder guide equation $y = (0.179x)^{0.5}$, $80 < x < 120$. Measurements were made on a diffractometer after sputtering.

Based on the results of fitting mirror reflection curves in „Multifitting“ program, the table lists the parameters of synthesized $Ni_{80}Mo_{20}/Si$ mirrors: period (d), reflection coefficient in the first Bragg diffraction order (R), the number of periods (N), the proportion of thickness of $Ni_{80}Mo_{20}$ in the period (β), $\sigma(Ni_{80}Mo_{20})$ and σ(Si) — the root-mean-square thickness of the transition region (the region of mixing materials and roughness of the layer interfaces) on the $Ni_{80}Mo_{20}$ and Si layers, respectively.

An example of the experimental and calculated mirror reflection curve from the KD-124 sample is shown in Fig. 2. It is possible to note a good agreement between the experimental reflection data and the fitting results for the model structure.

The table shows that the transition region thicknesses on the Si layers are larger than on the layers of $Ni_{80}Mo_{20}$. Some spread of the received data σ should be attributed to a fitting error. However, on average, $\sigma(Ni_{80}Mo_{20})$ is approximately equal to 5 Å, and σ(Si) is approximately equal to 8.5 Å. Perhaps this difference can be explained by the ballistic effect. That is, the heavier Ni and Mo atoms bombard the Si layer and penetrate to a greater depth. However, at this stage, it remains unclear what makes the main contribution to the transition region — interlayer roughness or mixing.

The theoretical models of mirror reflection curves were adjusted for one period of $d = 41.50$ Å taking into account the reconstructed interface thicknesses in the table. This step was made for a more correct comparison of the reflection coefficient values in the first diffraction order. Figure 3 shows the dependence of the reflection coefficient in the first Bragg peak as a function of the share of the thickness of $Ni_{80}Mo_{20}$ layer in the period. For comparison, the same figure shows the calculated values of the reflection coefficients in the case of perfectly smooth sharp interfaces of $Ni_{80}Mo_{20}/Si$ structure.

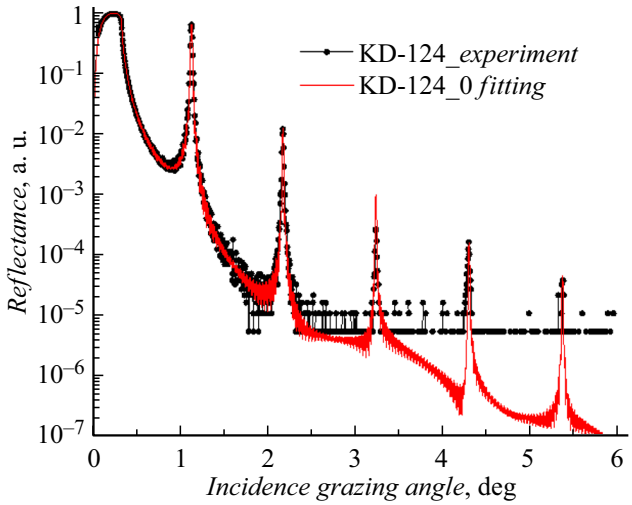

Figure 2. Fitting of the mirror reflection curve to the experimental data for the KD-124 sample.

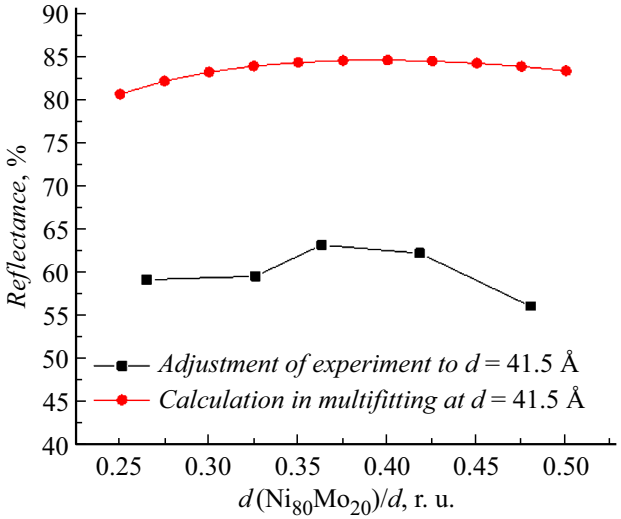

Figure 3. Reflection coefficient in the first order of diffraction depending on the share of the thickness of $Ni_{80}Mo_{20}$ layer in the period of $d = 41.50$ Å of structure of $Ni_{80}Mo_{20}/Si$.

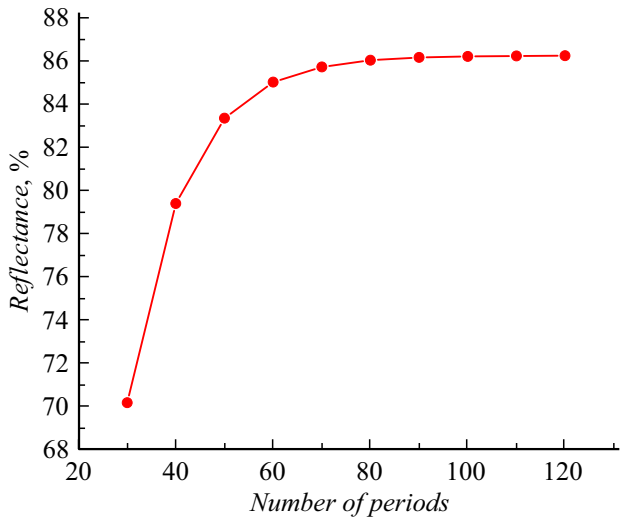

Figure 4. Calculated dependence of the reflection coefficient in the first diffraction order of $Ni_{80}Mo_{20}/Si$ structure with a period of $d = 41.50$ Å and a share of $Ni_{80}Mo_{20}$ in the period of $\beta = 0.40$.

It is possible to see from the graph in Fig. 3 that the optimal ratio of the thickness of $Ni_{80}Mo_{20}$ layer to the period thickness is in the range of $\beta \approx (0.36-0.42)$, which does not contradict the case of an ideal structure.

The structure with perfectly smooth and sharp boundaries was modelled in „Multifitting“ program to determine the optimal number of periods in a multilayer structure of $Ni_{80}Mo_{20}/Si$, which is necessary and sufficient to obtain the maximum reflection coefficient. The structure is based on the period of $d = 41.50$ Å and the proportion of $Ni_{80}Mo_{20}$ in the period of $\beta = 0.40$. Figure 4 shows a graph of the reflection coefficient versus the number of periods for the claimed structure.

The reflection coefficient in the first order of diffraction remains at 85.4% for the number of periods $N \geq 100$. Thus, one hundred periods will be a necessary and sufficient condition for achieving better reflectivity. It is important to determine this value from the point of view of technological feasibility. Of course, it is possible to sputter a known sufficient number of periods, for example, $N = 200$, to guarantee the maximum coefficient. However, a larger number of periods means a longer process time. During the process, parameters may drift (magnetron voltages, working gas pressure in the chamber, target and substrate temperature). Parameter drift will cause the period to drift and the reflection coefficient to decrease. Therefore, it is important to determine the optimal number of structure periods in advance.

Based on the simulation data, a multilayer structure $Ni_{80}Mo_{20}/Si$ with the number of periods $N = 100$ and $d \approx 41.50$ Å was synthesized. The mirror reflection curve is shown in Fig. 5, *a*. The first order of diffraction measured with greater accuracy is separately shown on Fig. 5, *b*.

The structural and reflective characteristics of the mirror are determined after fitting the data in Fig. 5: period of $d = 42.04$ Å, the proportion of $Ni_{80}Mo_{20}$ in period of $\beta = 0.401$, root-mean-square thicknesses of transition regions of $\sigma(Ni_{80}Mo_{20}) = 4.33$ and $\sigma(Si) = 9.87$ Å, reflection coefficient at the first Bragg peak of $R = 69.5\%$. Thus, $\sigma(Si) > \sigma(Ni_{80}Mo_{20})$ trend was maintained, and the reflection coefficient at optimal parameters reached almost 70%. The radiation reflection CuK_β at this angle was $R = 0.2\%$ based on the model of the spectral dependence of this structure constructed in „Multifitting“. Analogous models of synthesized W/Si structures for the period of $d \approx 40$ AA gave the reflection coefficients of the CuK_α and CuK_β lines at a given angle of $R = 71$ and 1%, respectively. That is, the suppression of CuK_β is 5 times stronger for the structure based on $Ni_{80}Mo_{20}$.

Next, the question of synthesizing a $Ni_{80}Mo_{20}/Si$ mirror with a period of $d \approx 33.5$ Å arose (another extreme value of periods on the parabola for the Goebel mirror). Models

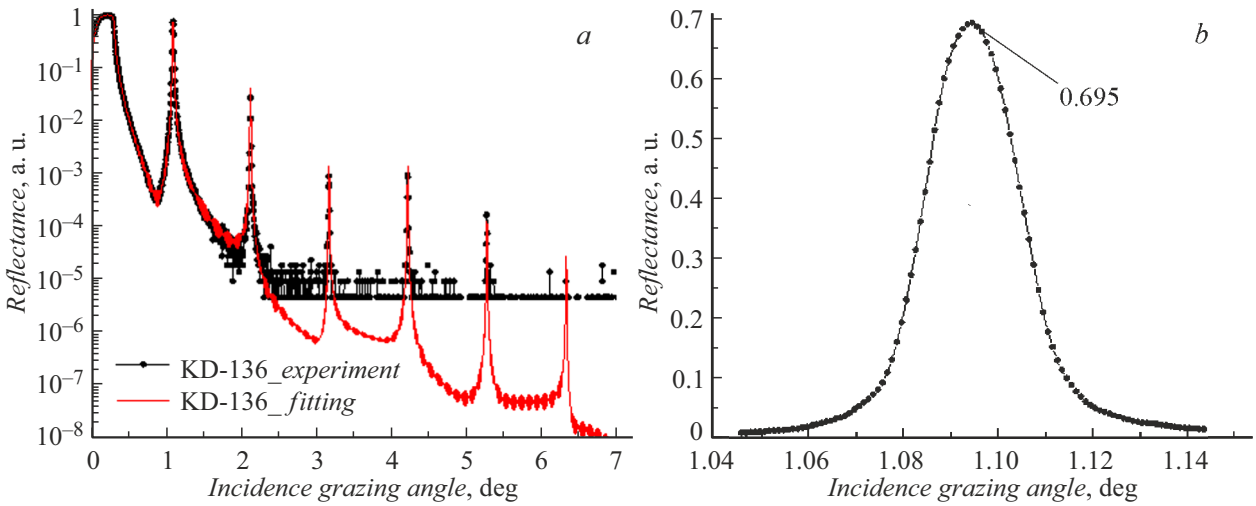

Figure 5. Specular reflection curve (*a*) and first order diffraction (*b*) of a multilayer structure $Ni_{80}Mo_{20}/Si$ with the number of periods $N = 100$ and the period of $d = 42.04$ Å.

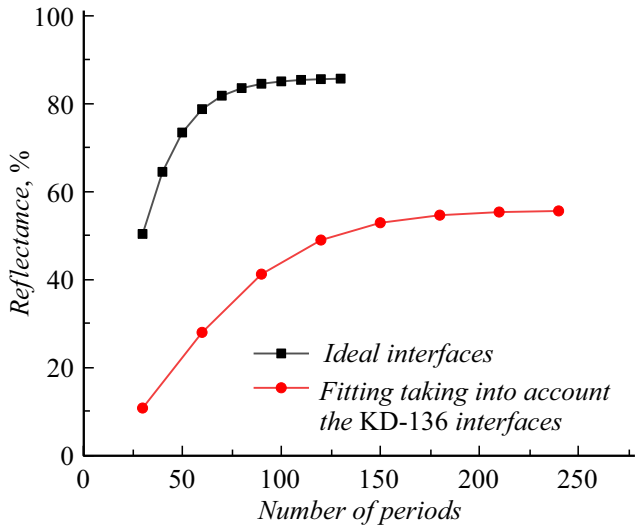

Figure 6. Dependence of the reflection coefficient in the first diffraction order on the number of layers of $Ni_{80}Mo_{20}$/Si structure with a period of $d = 33.5$ Å.

of reflection curves were constructed for this structure, taking into account the interface thicknesses reconstructed at the mirror with the period $d = 42.04$ Å, and also under the condition of ideal interfaces. After that, the graph of dependence $R(N)$ was plotted (Fig. 6).

For a mirror with a period of $d = 33.5$ Å and perfectly smooth sharp boundaries of $N = 100$ periods will be a necessary and sufficient condition for obtaining better reflective characteristics. However, given the actual rather large values of the transition regions, the number of periods will have to be increased to $N = 200$, according to the graph in Fig. 6. This is due to an increase of the extinction depth (i.e., the penetration of radiation deep into the structure). The presence of roughness results in a decrease of reflection at each boundary. Accordingly, the radiation penetrates further into the structure than in the case of ideal boundaries. The reflective layers enlarge.

The mirror reflection curve for $Ni_{80}Mo_{20}$/Si structure with $N = 200$ and $d \approx 33.5$ Å is shown in Fig. 7, *a*. The first order of diffraction measured with greater accuracy is separately shown on Fig. 7, *b*.

The fitting data in Fig. 7 were used to determine the structural and reflectance mirror characteristics: period $d = 32.09$ Å, share of $Ni_{80}Mo_{20}$ in period of $\beta = 0.417$, root-mean-square thicknesses of transition regions $\sigma(Ni_{80}Mo_{20}) = 6.40$ and $\sigma(Si) = 14.18$ Å, reflection coefficient in the first Bragg peak $R = 56.1\%$. The reflection of CuK_β radiation at this angle was $R = 0.03\%$ based on the model of the spectral dependence of this structure constructed in „Multifitting“. Analogous models of synthesized W/Si structures for the period of $d \approx 30$ AA gave the reflection coefficients of the CuK_α and CuK_β lines at a given angle of $R = 69$ and 0.2%, respectively. That is, the suppression of CuK_β is 6.5× stronger for the structure based on $Ni_{80}Mo_{20}$.

The transition region thicknesses of all synthesized structures remain quite large, which negatively affects their reflectivity. It is important to know which parameter affects the thickness of transition regions — root-mean-square roughness of interfaces or mixing of materials. This can help in the future when choosing a method for synthesizing structures to improve interfaces, which will suppress the development of a particular parameter.

The diffuse scattering curve shown in Fig. 8 was recorded to discriminate these contributions to the transition region for a sample of $Ni_{80}Mo_{20}$/Si with period of $d = 32.09$ Å.

Based on the structure model built in the „Multifitting“ program, the RMS values of interlayer roughnesses at both boundaries are $\sigma_e(Ni_{80}Mo_{20}) = \sigma_e(Si) = 0.35$ Å, i.e., mixing was the main contributor to the transition region.

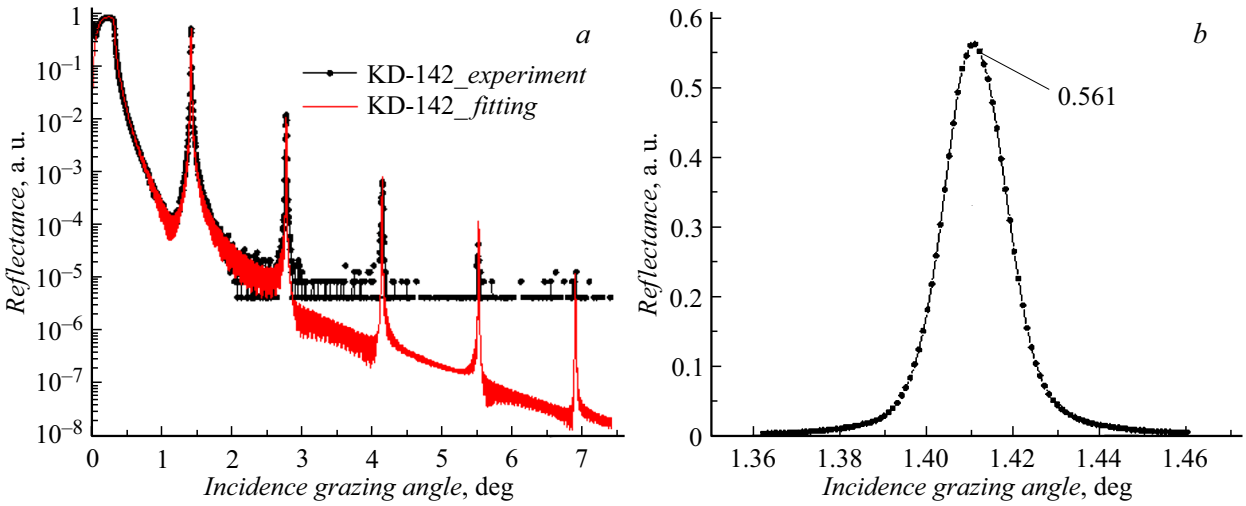

Figure 7. Specular reflection curve (*a*) and first order diffraction (*b*) of a multilayer structure $Ni_{80}Mo_{20}$/Si with the number of periods $N = 200$ and the period of $d = 32.09$ Å.

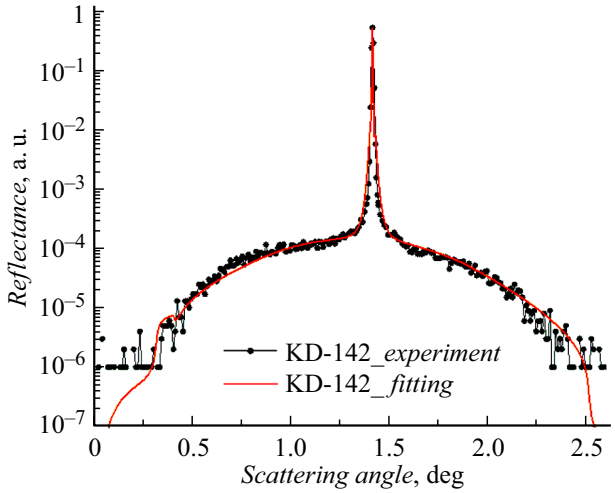

Figure 8. Experimental and calculated first-order diffuse scattering curve for a $Ni_{80}Mo_{20}$/Si sample with a period of $d = 32.09$ Å.

Conclusion

Optimal structural parameters were established in the course of this work, at which the reflective characteristics of $Ni_{80}Mo_{20}$/Si multilayer X-ray mirror had the best reflectivity within the framework of this technological sputtering process. The ratio of the thickness of $Ni_{80}Mo_{20}$ layer to the period thickness should be $\beta \approx (0.36-0.42)$.

The transition region thicknesses for all structures $\sigma(Ni_{80}Mo_{20})$ and $\sigma(Si)$ were ~ 5 and 8.5 Å accordingly. The trend $\sigma(Si) > \sigma(Ni_{80}Mo_{20})$ remains. The root-mean-square interlayer roughness at both boundaries was insignificant — $\sigma_e = 0.35$ Å. The layer mixing makes the main contribution to the thickness of the transition regions. Nevertheless, the reflectivity of multilayer structures $Ni_{80}Mo_{20}$/Si remained at an acceptable level ($R = 69.5-56.1\%$ for periods 41.5–32 Å), and in the future it is expected to increase application of methods for the synthesis of structures that inhibit the development of mixing of materials.

Funding

The study was supported financially by the Ministry of Science and Higher Education of the Russian Federation (agreement № 075-15-2021-1362).

Conflict of interest

The authors declare that they have no conflict of interest.

References

[1] M. Schuster, H. Göbel. J. Phys. D: Appl. Phys., **28**, 270 (1995). DOI: 10.1088/0022-3727/28/4A/053
[2] E. P. Kruglyakov, A.D. Nikolenko, E. P. Semenov, E. D. Chkhalo, N. I. Chkhalo. Poverkhnost. Rentgenovskie, sinkhrotronnye i neytronnye issledovaniya **1**, 151 (1999) (in Russian).
[3] D.L. Windt, F.E. Christensen, W.W. Craig, C. Hailey, F.A. Harrison, M. Jimenez-Garate, R. Kalyanaraman, P.H. Mao. J. Appl. Phys., **88** (1), 460 (2000).
[4] A.V. Andreev, A.G. Michette, A. Renwick. J. Modern Opt., **35**, 1667 (1988).
[5] O. Renner, M. Kopecký, E. Krouský, F. Schäfers, B.R. Müller, N.I. Chkhalo. Rev. Sci. Instrum., **63** (1), 1478 (1992). DOI: 10.1063/1.1143047
[6] M. Svechnikov. J. Appl. Crystallogr., **53** (1), 244 (2020).
[7] B.L. Henke, E.M. Gullikson, J.C. Davis. Atomic Data Nucl. Data Tables, **54** (2), 181 (1993).
[8] H. Takenaka, T. Kawamura, H. Kinoshita. Thin Solid Films, **288** (1–2), 99 (1996). DOI: 10.1016/S0040-6090(96)08837-2
[9] C. Sella, K. Youn, R. Barchewitz, M. Arbaoui, R. Krishnan. Appl. Surf. Sci., **33–34**, 1208 (1988). DOI: 10.1016/0169-4332(88)90436-9
[10] M. Cilia, J. Verhoeven. J. Appl. Phys., **82**, 4137 (1997). DOI: 10.1063/1.366213
[11] D.G. Stearns. Appl. Phys. Lett., **62** (15), 1745 (1993).
[12] G. Palasantzas. Phys. Rev. B, **48** (19), 14472 (1993).

Translated by A.Akhtyamov